

Neutron Flux Underground Revisited

H. Wulandari ^{*}, J. Jochum, W. Rau, F. von Feilitzsch

*Physikdept. E-15, Technische Universität München, James-Franckstr.-
85747 Garching, Germany*

Abstract

The neutron flux induced by radioactivity at the Gran Sasso underground laboratory is revisited. We have performed calculations and Monte Carlo simulations; the results offer an independent check to the available experimental data reported by different authors, which vary rather widely. This study gives detailed information on the expected spectrum and on the variability of the neutron flux due to possible variations of the water content of the environment.

Key words: Neutron; Underground site; Spontaneous fission; (α, n) reactions

PACS: 25.85.Ca; 28.20-v; 29.25.Dz

1 Introduction

One of the important parameters characterizing an underground environment is the neutron flux. Recently, the role of neutrons as a source of background has received more attention. Estimates of the neutron flux from surrounding materials are needed for rare event searches in underground sites. Highly sensitive underground neutrino experiments require precise knowledge of neutron-induced background in the detector. In direct searches for WIMP dark matter neutrons are a particularly important background, because they interact with the detector in the same way WIMPs do.

The dominant sources of neutrons at large depth underground, where the cosmic rays are reduced significantly, are the (α, n) reactions on light elements (e.g. Li, F, Na, etc.) and the spontaneous fission, mainly of ^{238}U . In general, at a depth of 3000 – 4000 m w.e., where many rare event experiments are located, the flux of neutrons from activity of the experimental environment

^{*} Corresponding author. Tel: +49-89-28914416, Fax: +49-89-28912680.

Email address: Hesti.Wulandari@ph.tum.de (H. Wulandari).

is two to three orders of magnitudes higher than the flux of neutrons from cosmic ray muons.

Due to its very low intensity, the neutron flux underground is not easy to measure. At the Gran Sasso underground laboratory the neutron flux has been measured by several groups, employing different methods of detection [1,2,3,4,5,6]. To get the neutron flux from the measurements, Monte Carlo simulations are usually performed, because the parameters required to handle the experimental data (detector efficiency, energy spectrum of the incoming neutrons, etc.) are usually unknown or difficult to determine experimentally. Table 1 summarizes the results of the neutron flux measurements at the Gran Sasso laboratory. One measurement was performed in hall C by the ICARUS collaboration [2], while all others were performed in hall A of the laboratory. Most of the measurement results are given as the integral flux in a large energy bin. Although different energy binning was used in these measurements, one can see that the results vary rather widely. Only two measurements [2,3] give some information on the spectral shape. However, for some purposes a more detailed spectrum is needed.

The total flux of [2] is basically consistent with the result of [3] for $E > 1$ MeV, while the energy spectrum as a whole is significantly harder. The results from [2] show important distortions with respect to the spectrum that was previously generally assumed in literature, i.e. a spectrum produced mainly by spontaneous fission. The difference is seen at high energies. To search for a possible explanation the authors of [2] considered the production of neutrons via (α, n) reactions inside the rock and computed the 'thin target' spectrum of neutrons produced by the reaction $^{17}\text{O}(\alpha, n)^{20}\text{Ne}$ only. The (α, n) and spontaneous fission spectra were then used as input for the MCNP (Monte Carlo N-Particles) code to obtain the effective neutron flux in hall C. They found that their measurements and simulations are in very good agreement and that (α, n) reactions are the main source of the high energy neutron flux in the laboratory. However, according to [7] the uncertainties quoted in [2] have been underestimated. They should be multiplied by $\sqrt{3}$ to get the proper uncertainties, due to the fact that the background run in this experiment is about three times shorter than the data run. Then all data points shown in [2] would be insignificant and the agreement between the thin target calculation and the measurement found here would be merely accidental.

Based on Monte Carlo simulations, this work is devoted to reinvestigate the neutron flux from (α, n) and fission reactions in the rock and concrete of the Gran Sasso laboratory. The results offer an independent check to the present experimental data and give detailed information on the shape of the spectrum.

2 Calculation of Neutron Production by (α, n) and Fission Reactions in the Rock and Concrete

2.1 Composition and Activity of the Rock and Concrete

Gran Sasso rock consists mainly of CaCO_3 and MgCO_3 , with a density of $2.71 \pm 0.05 \text{ g/cm}^3$ [8]. The weight percentage of the elements is given in Table 2. Due to the presence of a certain type of rock, called “roccia marnosa nera”, the contaminations of ^{238}U and ^{232}Th in hall A rock are about ten and thirty times higher respectively than those of hall C [4] as shown in Table 3.

Since there are no data on the chemical composition of Gran Sasso concrete available in literature, several samples were taken from different places in the laboratory. The concrete samples were then analyzed at the laboratory of the *Lehrstuhl für Baustoffkunde und Werkstoffprüfung* at the department of civil engineering of the Technische Universität München. No significant variations were found in the chemical composition of the samples, which leads to the conclusion that all halls in Gran Sasso are layered with the same type of concrete. The typical water content in the concrete is 12%, with a possible variation of 4% at most (in most cases the variation is smaller). The weight percentage of elements in concrete with 8% water content (hereafter “dry concrete”) is shown in Table 4. The ^{238}U and ^{232}Th contaminations are $1.05 \pm 0.12 \text{ ppm}$ and $0.656 \pm 0.028 \text{ ppm}$ [9] respectively. The density is between 2.3 and 2.5 g/cm^3 , depending on the assumed water content.

2.2 Neutron Production by Spontaneous Fission

There are mainly three nuclides in nature that undergo spontaneous fission: ^{238}U , ^{235}U and ^{232}Th . Only neutrons produced by spontaneous fission of ^{238}U are considered here, because of the long fission half life of the other two nuclides compared to that of ^{238}U . The spectrum of the emitted neutrons follows the Watt spectrum:

$$N(E) = C \exp(-E/a) \sinh(bE)^{1/2} \quad (1)$$

In this work the Watt spectrum parameters of the Los Alamos model results [10] have been used, where $a = 0.7124 \text{ MeV}$ and $b = 5.6405 \text{ MeV}^{-1}$. The rate of spontaneous fission of ^{238}U is $0.218/\text{year/g}$ of rock (concrete) for 1 ppm of ^{238}U and the average number of neutrons emitted per fission event is 2.4 ± 0.2 [11]. This gives $0.52 \text{ neutrons/year/g}$ of rock (concrete)/ppm ^{238}U . This number multiplied by the ^{238}U activities in the rock/concrete would give 3.54,

0.22 and 0.34 neutrons/year/g in the rock of hall A, B and C respectively and 0.55 neutrons/year/g in the concrete. Figure 1 shows the neutron energy distribution due to spontaneous fission of ^{238}U .

2.3 Neutron Production by (α,n) Reactions

Uranium, thorium, and their daughter products decay by emitting α and β particles. In the rock (concrete) α -particles can interact especially with light elements and produce neutrons through (α,n) reactions.

The yield of neutrons per α -particle for an individual element depends on the (α,n) interaction cross section (which is energy dependent), and on the energy loss of α -particles in a medium made of that element. In this work the thick target yield of (α,n) reactions was used instead of the thin target yield used in [2]. The thick target yield of the (α,n) reaction for an individual element j in which the α -particle has a range R can be written as [12]:

$$Y_j = \int_0^R n_j \sigma_j(E) dx \quad (2)$$

where n_j is the number of atoms per unit volume of element j , and σ_j is the microscopic (α,n) reaction cross section for an α -particle energy E . Transforming the right side of Eq. 2 into an integral over energy gives:

$$\begin{aligned} Y_j &= \int_0^{E_i} \frac{n_j \sigma_j(E)}{-(dE/dx)} dE \\ &= \int_0^{E_i} \frac{n_j \sigma_j(E)}{\rho_j S_j^m(E)} dE \\ &= \int_0^{E_i} \frac{n_j \sigma_j(E) N_A}{n_j A_j S_j^m(E)} dE \\ &= \frac{N_A}{A_j} \int_0^{E_i} \frac{\sigma_j(E)}{S_j^m(E)} dE \end{aligned} \quad (3)$$

where E_i is the initial α -energy, N_A is the Avogadro number, A_j is the atomic mass and σ_j and S_j^m are the (α,n) cross section and the mass stopping power respectively, which are energy dependent.

Neutron yields from individual elements can be used to calculate the total yield in a chemical compound or mixture [12,13,14]. The following assumptions are

usually made in such a calculation:

- (i) the compound is a homogeneous mixture of its constituent elements
- (ii) Bragg's law of additivity for stopping power holds for the compound
- (iii) the ratio of an element's stopping power to the total stopping power of the compound is independent of the α -particle energy.

The validity of (iii) has been discussed by several authors. Although for each element the mass stopping power S_j^m decreases with energy, Feige [12] found that the mass stopping power ratio for any pair of elements does not change by more than $\pm 4\%$ between 5.3 MeV and 8.8 MeV. Heaton *et al.* [15] showed that above 3 MeV this approximation introduces an uncertainty of less than 5% in the neutron yield.

Under those assumptions the neutron yield of element j in the compound or mixture with initial α -particle energy E_i can be written as:

$$\begin{aligned}
 Y_{i,j,mix} &= \int_0^{E_i} \frac{n_j \sigma_j}{\sum_j \rho_j S_j^m} dE \\
 &= \int_0^{E_i} \frac{\rho_j S_j^m}{\sum_j \rho_j S_j^m} \frac{n_j \sigma_j(E)}{\rho_j S_j^m} dE \\
 &= \frac{\rho_j S_j^m(E_0)}{\sum_j \rho_j S_j^m(E_0)} \int_0^{E_i} \frac{n_j \sigma_j(E)}{\rho_j S_j^m} dE \\
 &= \frac{M_j S_j(E_0)}{\sum_j M_j S_j(E_0)} Y_j(E_i)
 \end{aligned} \tag{4}$$

where M_j is the mass fraction of element j in the mixture, E_0 is a chosen reference energy (8 MeV in this work), S_j^m is the mass stopping power and $Y_j(E_i)$ is the neutron yield of element j in isolation (see Eq. (3)). Thus the (α,n) yield of a compound (mixture) is the sum of the yields of its elements weighted by the relative contributions of the elements to the total stopping power of the compound. The use of 8 MeV mass stopping power was selected because the overwhelming contribution to the neutron yield comes from high energy α -particles and the relative stopping power of elements are nearly independent of the α -energy in this energy region [16]. The mass stopping powers at 8 MeV of elements used in this work are as those used in [15]. In this work the data on neutron yield of elements in isolation, in units of neutron/ α , is taken from a compilation by Heaton *et al.* [16,17].

Each α emitter in the ^{238}U and ^{232}Th decay chains emits α 's at a certain energy, which was used as the initial energy in the neutron yield calculation. The neutron yield of each element with certain initial energy was then multiplied

by the branching ratio, the number of α 's emitted by each emitter per unit time, and the concentration of ^{238}U and ^{232}Th in the rock (concrete). It is assumed in this work, that ^{238}U and ^{232}Th are in secular equilibrium with their daughter products. The total neutron production rate for each element was calculated by summing up the contribution of all alpha emitters.

In Table 5 and Table 6 neutrons produced per unit mass per year by (α, n) reactions with the elements of the rock in hall A, hall C and also in dry concrete are presented. It is seen that fission (see discussion in the previous section) and (α, n) reactions contribute more or less equally to the total production rates both in the rock and in the concrete. Half of the total (α, n) neutron production in the rock comes from interactions of α particles with magnesium, which comprises only less than 6% of the weight percentage of the rock, whereas oxygen with almost 50% weight percentage contributes to only about 20% of the production rate. Due to the higher activity of the hall A rock the (α, n) neutron production in the rock of this hall is more than ten times higher than in the hall C rock. In the concrete Na, Al and Mg contribute significantly in spite of their minor weight percentages. The production rate per unit mass in the wet concrete is slightly smaller than in the dry concrete, but this is merely due to the difference in the densities. The volume of concrete remains, while the mass changes with the water content. Given per unit volume the production rates in dry and wet concrete are the same.

The energy of the emitted neutron is dependent on the α energy, the reaction energy Q , and the neutron emission angle. It was calculated under the following assumptions:

- (i) the interaction take place at the initial α energy
- (ii) the neutron is emitted at 90°
- (iii) the residual nucleus is produced in its ground state.

Under these assumptions, neutron energy can be determined by using simple Eq. (5):

$$E_n = \frac{MQ + E_\alpha(M - M_\alpha)}{(M_n + M)} \quad (5)$$

Here M is the mass of the final nucleus, M_n and M_α are the masses of neutron and the α particle respectively, and E_α is the initial α energy.

The threshold energy E_{th} for an (α, n) reaction is the minimum kinetic energy the impinging α particle must have (in the laboratory system) in order to make the reaction energetically possible. For endothermic reactions, the threshold energy is:

$$E_{th} = -[(M_n + M_\alpha)/M_1]Q \quad (6)$$

where M_1 and M_α are the masses of the target nucleus and of α particle respectively. The threshold energy is zero for exothermic reactions, i.e. reactions with positive Q .

The highest energy among naturally emitted α particles is 8.79 MeV, which comes from the decay of ^{212}Po . Hence, for some elements in the rock/concrete there are isotopes that can not participate in the (α, n) reactions, because of their high E_{th} (e.g. ^{16}O , ^{28}Si , ^{24}Mg , and ^{40}Ca). For each element calculations of neutron energies were therefore done for all isotopes that are not closed for (α, n) interactions. Then, neutron mean energies of elements were calculated according to the relative abundances of the “open” isotopes for different α energies. Finally, the yields of all elements were summed up in 0.5 MeV energy bins to get the energy spectra of neutrons from (α, n) reactions as shown in Figure 2 for hall A rock, hall C rock, and dry concrete. Neutrons with energy above 6 MeV are contributions of magnesium and carbon. While neutrons below 4 MeV are mainly produced by spontaneous fission, (α, n) reaction is the main contributor in the production of neutrons with energy above 4 MeV.

3 Flux of (α, n) and Fission Neutrons at LNGS

To get the flux of low energy neutrons inside the halls, the Monte Carlo code MCNP4B (Monte Carlo N-Particles version 4B) from Los Alamos [18] was used to transport neutrons produced by fission and (α, n) reactions as calculated above through the rock and concrete and scatter them inside the halls.

Table 7 summarizes the typical depths of neutrons (the depths where $\sim 63\%$ of neutrons come from, the $1/e$ length) produced in hall A rock and in dry concrete, and entering hall A (before scattering inside the hall) with any energy and in addition with energy $E > 1$ MeV. Neutrons with $E > 1$ MeV come mainly from the first 7 cm and 13 cm of concrete and rock respectively. As the thickness of the concrete layer in Gran Sasso is not less than 30 cm (in some places even around 1 m), the bulk of the total flux in the laboratory is given by neutrons produced in the concrete.

In the further simulations performed to get the neutron flux inside the halls, the thickness of the concrete layer in the laboratory has been set to 45 cm below the floor and 35 cm elsewhere, and 2 m of rock have been taken into account. The calculated fluxes of neutrons (after scattering inside the halls) are shown in Table 8 for hall A with 8% (dry) and 16% (wet) water content in the concrete, for hall C with dry concrete, together with the measurement in Hall A by Belli et al. [3] as a comparison. The measured flux between 1 – 2.5 MeV is taken from [2]. We calculated the errors in this energy bin by assuming that the errors in 1 keV – 1 MeV and 1 – 2.5 MeV bins are equal. In our work, errors

can be induced mainly by the uncertainties in the data (compositions and activities of rock and concrete, neutron yield for individual elements, stopping power), which are mostly not available, and the assumptions used to calculate the neutron production rates. It is not easy therefore, to estimate the overall errors for our results. The statistical errors for the simulations are relatively easy to suppress and are a minor contributor to the total errors.

The total flux and the integral flux above 1 MeV in hall A are consistent with those of the measurement if the concrete in hall A is dry. The simulated flux differs from the measured one in the chosen bins below 1 MeV. In our simulations we have assumed that there is nothing inside the hall and neutrons can only be scattered by the walls. In reality as in the measurement, neutrons coming from the rock/concrete can be scattered by anything inside the hall before they eventually come into the experimental setup. Those neutrons are being moderated, raising the flux in the lowest energy bin.

For the case of dry concrete, the total flux in hall C is only about 40% less than in hall A, although the neutron production rate in hall C rock is more than ten times lower than that of hall A. Above 1 MeV the difference is even only 20%. The concrete indeed reduces the neutron flux from the rock significantly and neutrons coming into the halls are mainly those produced in the concrete layer.

Table 8 shows that the neutron flux depends on the humidity of the environment. The flux in Hall A is lower if the concrete is wet than if it is dry. As mentioned in the previous section, the 8% difference in the water content of concrete does not lead to different neutron production rates. The effect seen in the flux here is caused only by moderation. Wet concrete moderates neutrons more effectively than dry concrete due its higher hydrogen content. The fluxes obtained for dry and wet concrete (8% and 16% water content respectively) here show the maximum possible variation for the water content of concrete. A more realistic variation of water content ($12 \pm 1\%$) results consequently in smaller flux variation. To quantify this effect and to see whether it is a seasonal phenomena, one needs to monitor the water content of the concrete for at least one year.

Detailed spectra of neutrons in hall A and hall C are shown in Figure 3 for neutron energy above 0.5 MeV. Each point shows the integral flux in a 0.5 MeV energy bin. The contribution of (α, n) makes the spectra in both halls differ from the spectrum expected for neutrons produced by fission reactions only, especially at high energies.

4 Conclusion

We have discussed the flux of neutrons induced by radioactivity in the rock and concrete surrounding the Gran Sasso laboratory. The flux is dominated by neutrons produced in the concrete layer and therefore does not vary much from hall to hall. A more detailed spectrum compared to that from measurements has been obtained. The spectrum differs from the spectrum expected for neutron produced by fission reactions only, especially at high energies due to the contribution of (α, n) neutrons. We also have shown the dependence of the neutron flux on the humidity of the concrete. Our results for the case of hall A with dry concrete are in good agreement with the experimental data from [3].

5 Acknowledgement

H. Wulandari thanks the *Deutscher Akademischer Austausch Dienst* (DAAD) for the financial support of her PhD work.

References

- [1] R. Aleksan et al., Nucl. Inst. Meth. in Phys. Res. A 274 (1989) 203.
- [2] F. Arneodo et al., Il Nuovo Cim. 112 A, N.8 (1999) 819.
- [3] P. Belli et al., Il Nuovo Cim. 101 A, N.6 (1989) 959.
- [4] E. Bellotti et al., INFN/TC-85/19, October 1985.
- [5] M. Cribier et al., Astropart. Phys. 4 (1995) 23.
- [6] A. Rindi, F. Celani, M. Lindozzi and S. Miozzi, Nucl. Inst. Meth. in Phys. Res. A 272 (1988) 871.
- [7] G. Gerbier, private communication.
- [8] P.G. Catalano et al., Mem. Soc. Geol. It., 35 (1986) 647.
- [9] G. Bellini et al., Borexino Proposal to Gran Sasso Laboratory, (1991) 184.
- [10] D. Madland, private communication.
- [11] D.J. Littler, Proc. Phys. Soc. London A 64 (1951) 638; A 65 (1952) 203.
- [12] Y. Feige, B.G. Oltman, and J. Kastner, Journal of Geophys. Research Vol. 73, No. 10 (1968) 3135.

- [13] D. West, Ann. Nucl. energy 6 (1979) 549.
- [14] V.I. Bulanenko, V.V. Frolov, and É.M. Tsenter, At. Energ. 53 (1982) 160.
- [15] R. Heaton, H. Lee, P. Skensved, and B.C. Robertson, Nucl. Geophys. 4 N.4, (1990) 499.
- [16] R. Heaton, H. Lee, P. Skensved, and B.C. Robertson, Nucl. Inst. Meth. in Phys. Res. A276 (1989) 529.
- [17] R. Heaton, private communication.
- [18] J.F. Briesmeister, Ed., “MCNP-A General Monte Carlo N-Particle Code, Version 4B”, LA-12625-M, Los Alamos National Laboratory (March 1997).

Table 1

Neutron flux measurements at Gran Sasso laboratory reported by different authors. In analyzing their experimental data with Monte Carlo simulations, Belli et al. [3] have used two different hypothetical spectra: flat, and flat plus a Watt fission spectrum. This leads to the upper and lower data sets shown for ref. [3] respectively.

E interval (MeV)	Neutron Flux ($10^{-6}\text{cm}^{-2}\text{s}^{-1}$)								
	Ref. [1]	Ref. [2]	Ref. [3]	Ref. [4]	Ref. [5]	Ref. [6]			
$10^{-3} - 0.5$	0.78±0.3		0.54±0.01 (0.53±0.08)		3.0±0.8 0.09±0.06	2.56±0.27			
0.5 – 1									
1 – 2.5		0.14±0.12							
2.5 – 3		0.13±0.04	0.27±0.14 (0.18±0.04)						
3 – 5		0.15±0.04	0.05±0.01 (0.04±0.01)						
5 – 10									
10 – 15		$(0.4 \pm 0.4) \cdot 10^{-3}$	$(0.6 \pm 0.2) \cdot 10^{-3}$ $((0.7 \pm 0.2) \cdot 10^{-3})$						
15 – 25			$(0.5 \pm 0.3) \cdot 10^{-6}$ $((0.1 \pm 0.3) \cdot 10^{-6})$						

Table 2

Chemical composition of LNGS rock.

Element	C	O	Mg	Al	Si	K	Ca
% Weight	11.88	47.91	5.58	1.03	1.27	1.03	30.29

Table 3

^{238}U and ^{232}Th activities in LNGS rock.

Hall	Activities (ppm)	
	^{238}U	^{232}Th
A	6.80	2.167
B	0.42	0.062
C	0.66	0.066

Table 4

Chemical composition of LNGS dry concrete.

Element	H	C	O	Na	Mg	Al	Si	P	S	K	Ca	Ti	Fe
% Weight	0.89	7.99	48.43	0.6	0.85	0.9	3.86	0.04	0.16	0.54	34.06	0.04	0.43

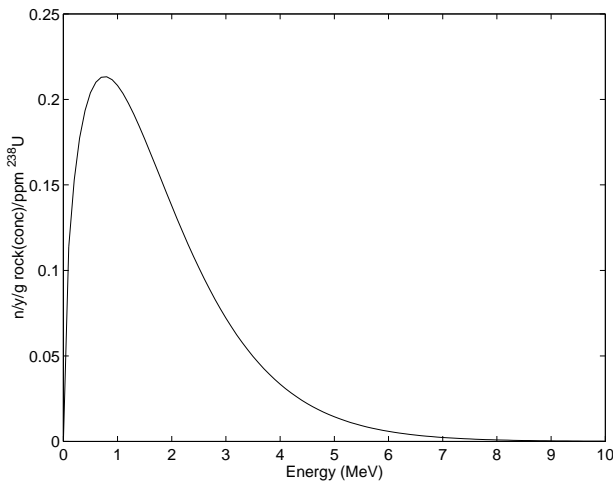


Fig. 1. Energy spectrum of neutrons from spontaneous fission of ^{238}U .

Table 6

Neutron yields from (α, n) interactions in dry concrete (8% water content).

Table 5
Neutron yields from (α, n) interactions in the rock.

Element	Total elemental yield (n/y/g rock)	
	Hall A	Hall C
C	4.60E-1	4.07E-2
O	8.8E-1	7.90E-2
Mg	2.31E+0	2.04E-1
Al	3.50E-1	3.05E-2
Si	6.00E-2	5.21E-3
K	9.00E-2	7.60E-3
Ca	2.40E-1	2.05E-2
Total yield	4.38E+0	3.88E-1

Element	Total elemental yield (n/y/g conc.)
C	5.24E-2
O	1.50E-1
Na	9.65E-2
Mg	6.07E-2
Al	5.35E-2
Si	3.16E-2
P	4.35E-4
S	3.36E-4
K	8.31E-3
Ca	4.95E-2
Ti	3.35E-4
Fe	9.53E-4
Total yield	5.05E-1

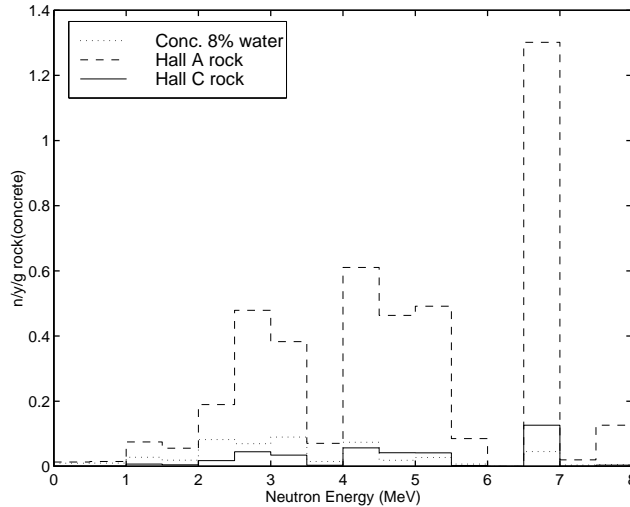


Fig. 2. Energy spectra of neutrons from (α, n) reactions as used in the simulations.

Table 7

Typical depths (in cm) of (α, n) and fission neutrons produced in hall A rock and dry concrete. “Energy” represents the energy of neutrons entering hall A before scattering in the hall.

Energy	Hall A rock		Dry concrete	
	Fission	(α, n)	Fission	(α, n)
all energy	23	24	10.5	12
> 1 MeV	10	13	6.5	6.5

Table 8

Simulated neutron flux in hall A with dry (8% water content) and wet (16% water content) concrete, in hall C with dry concrete and the measurements by Belli et al. [3] for the two hypothetical spectra mentioned in Table 1.

Energy (MeV)	Neutron Flux ($10^{-6} n/cm^2 s$)				
	Measurement in hall A [3]		MC Simulations, this work		
	Flat	Flat+Watt Spect.	Hall A,dry	Hall A,wet	Hall C,dry
$0 - 5.10^{-8}$	1.08 ± 0.02	1.07 ± 0.05	0.53	0.24	0.24
$5.10^{-8} - 10^{-3}$	1.84 ± 0.20	1.99 ± 0.05	1.77	0.71	0.93
$10^{-3} - 2.5$ (1 - 2.5)	0.54 ± 0.01 (0.38 ± 0.01) ¹	0.53 ± 0.08 (0.38 ± 0.06) ^{1,2}	1.22 (0.35)	0.57 (0.18)	0.91 (0.27)
$2.5 - 5$	0.27 ± 0.14	0.18 ± 0.04	0.18	0.12	0.15
$5 - 10$	0.05 ± 0.01	0.04 ± 0.01	0.05	0.03	0.03
Total Flux Flux($E > 1$ MeV)	3.78 ± 0.25	3.81 ± 0.11	3.75	1.67	2.26
	0.70 ± 0.14	0.60 ± 0.07	0.58	0.33	0.45

¹Taken from [2]. ²Errors are assumed to be equal below and above 1 MeV.

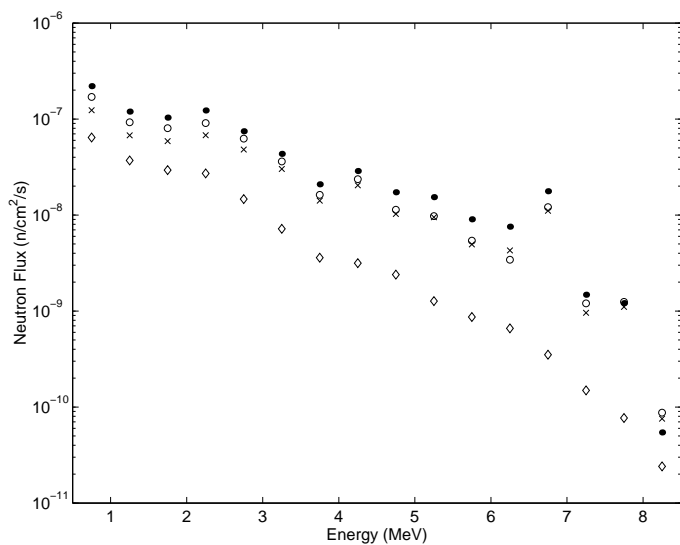


Fig. 3. Neutron flux at the Gran Sasso laboratory, ●: hall A, dry concrete, X: hall A, wet concrete, ◇: hall A, fission reactions only and ○: hall C, dry concrete. Each point shows the integral flux in a 0.5 MeV energy bin.